# NMR of solutes in nematic and smectic A liquid crystals: The anisotropic intermolecular potential

**ARTICLE** *in* MAGNETIC RESONANCE IN CHEMISTRY · AUGUST 2014

Impact Factor: 1.18 · DOI: 10.1002/mrc.4113



**4 AUTHORS**, INCLUDING:

Ronald Y Dong

University of British Columbia - Vancouver

**220** PUBLICATIONS **2,270** CITATIONS

SEE PROFILE

Adrian Weber

University of Winnipeg

**22** PUBLICATIONS **134** CITATIONS

SEE PROFILE

Anand Yethiraj

Memorial University of Newfoundland

**62** PUBLICATIONS **1,256** CITATIONS

SEE PROFILE

Special issue mini-review

MRC

Received: 29 April 2014 Revised: 19 June 2014 Accepted: 29 June 2014 Published online in Wiley Online Library

(wileyonlinelibrary.com) DOI 10.1002/mrc.4113

# NMR of solutes in nematic and smectic A liquid crystals: the anisotropic intermolecular potential

**E. Elliott Burnell,[a]* Ronald Y. Dong,[b] Adrian C. J. Weber[c] and Anand Yethiraj[d]**

**Orientational order parameters determined from $^1$H NMR spectroscopy of solutes in liquid crystals that form both nematic and smectic A phases are used to determine the solute smectic A order parameters and the smectic–nematic coupling term. For the analysis, it is necessary to know the nematic part of the potential in the smectic A phase: various ways of extrapolating parameters from the nematic phase to the smectic phase are explored. Copyright © 2014 John Wiley & Sons, Ltd.**

**Keywords:** NMR; $^1$H; liquid crystal; nematic; smectic; solute; anisotropic; intermolecular potential; order parameter

## Introduction

Liquid crystals form a wide variety of different phases, with the simplest being the nematic (N) phase, which is characterized by the orientational order of the molecules that comprise the phase. The average direction of the molecules defines the director. The molecules of smectic phases possess positional order in addition to the N orientational order, with the simplest being the smectic A (SmA) phase for which the N director is perpendicular to the smectic layers.[1] The precise nature of the anisotropic intermolecular forces that give rise to the orientational and positional order has been a topic of much interest.

Many different physical techniques have been used to investigate these ordered fluids, with NMR being one of the most important. The NMR spectra of these orientationally ordered fluids are dominated by the anisotropic dipolar, quadrupolar and chemical shift anisotropy interactions. The interaction parameters obtainable from the analysis of the NMR spectra give information on the extent of orientational order, and this orientational order is in turn related to the anisotropic intermolecular interactions that are responsible for the liquid crystallinity.[2,3]

One problem associated with the use of NMR parameters obtained from the liquid-crystal molecules themselves is that they are not the axially symmetric particles assumed in Maier–Saupe (MS) theory,[4,5] and they normally exist in multiple different, symmetry-unrelated conformers making precise analysis difficult and fraught with assumptions. Hence, the information obtained is a function of the approximations made. One very successful approach has involved the use of small solutes as probes of the anisotropic environment.[6–10] It is normal to choose 'rigid', well-characterized solutes of relatively high symmetry, thus simplifying spectral analysis and yielding the solute molecular order parameter matrix with essentially no assumptions.

The SmA phase is characterized by positional (in addition to orientational) order, but the NMR observables do not provide direct information on this positional order. Unlike the N orientational order parameters, which are directly proportional to the dipolar couplings obtained from the analysis of the NMR spectra of solutes, as we shall see later in the text, the SmA parameters cannot be unambiguously obtained from the spectral parameters.

Here, we review our attempts to obtain smectic positional order information for solutes using the orientational order parameters obtained from their $^1$H NMR spectra as a function of temperature (spanning N and smectic ranges of the phase diagram) and of liquid-crystal composition. We shall build the story starting with the evidence that the NMR results do indicate the formation of SmA phases, and shall describe the various ways we have used to extract information about the SmA prefactors. We concentrate on results for the single solute, 1,4-dichlorobenzene (pdcb). The main problem is how to describe the N (i.e. orientational) potential in the SmA phases. In order to deal with this, we assume that we can extrapolate or interpolate parameters describing the N potential from the N into the SmA phase, and we explore several different ways of doing this.

## Review of Theory

### Nematic phase: liquid-crystal molecules

For a collection of axially symmetric liquid-crystal molecules, the liquid-crystal second-rank order parameter $S_L$ describes the orientational order and is defined by

* *Correspondence to: E. Elliott Burnell, Chemistry Department, University of British Columbia, 2036 Main Mall, Vancouver, BC, V6T 1Z1, Canada. E-mail: elliott.burnell@ubc.ca*

a *Chemistry Department, University of British Columbia, 2036 Main Mall, Vancouver, BC, V6T 1Z1, Canada*

b *Physics Department, University of British Columbia, 6224 Agricultural Road, Vancouver, BC, V6T 1Z1, Canada*

c *Chemistry Department, Brandon University, 270 18th Street, Brandon, MB, R7A 6A9, Canada*

d *Department of Physics and Physical Oceanography, Memorial University, St. John's, NL, A1B 3X7, Canada*

$$S_L = \frac{\int \left(\frac{3}{2}\cos^2\theta_L - \frac{1}{2}\right) e^{-\frac{\mathscr{H}_{N,L}(\theta_L)}{k_B T}} \sin\theta_L d\theta_L}{\int e^{-\frac{\mathscr{H}_{N,L}(\theta_L)}{k_B T}} \sin\theta_L d\theta_L} \quad (1)$$

where $\mathscr{H}_{N,L}(\theta_L)$ is the average field experienced by the liquid-crystal molecule and $\theta_L$ is the angle between the molecular symmetry axis and the director. Even though most molecules that comprise N phases are far from axially symmetric, it is usual to assume axial symmetry and to use Eqn (1).

The MS mean-field theory[4,5] of such axially symmetric particles provides the classic and simple relationship for $\mathscr{H}_{N,L}(\theta_L)$

$$\mathscr{H}_{N,L}(\theta_L) = -\nu S_L \left(\frac{3}{2}\cos^2\theta_L - \frac{1}{2}\right) \quad (2)$$

where $\nu$ gives the strength of the liquid-crystal mean field, which is modulated by the order parameter. The interaction strength of a particle with the mean field varies with angle $\theta_L$ between symmetry and mean-field directions *via* the $P_2(\cos\theta_L) = \left(\frac{3}{2}\cos^2\theta_L - \frac{1}{2}\right)$ term.

### Smectic A phase: liquid-crystal molecules

In addition to orientational order, the molecules that make up smectic phases also have positional order, with the simplest example being the SmA phase. A classic description of this positional order is given by Kobayashi–McMillan (KM) theory, which adds two parameters to the MS theory for nematics, being a sinusoidal positional probability characterized by $\tau_L'$ and a sinusoidal variation of the N potential throughout a layer, characterized by the coupling term $\kappa_L'$[11,12]

$$\mathscr{H}_{SmA,L}(\theta_L, Z) = \mathscr{H}_{N,L}(\theta_L)\left[1 + \kappa_L' \cos\left(\frac{2\pi Z}{d}\right)\right] - \tau_L' \cos\left(\frac{2\pi Z}{d}\right) \quad (3)$$

where $d$ is the layer thickness and $Z$ the position within the layer. An important aspect to the understanding of such phases involves understanding of the anisotropic intermolecular forces that are at play.

### Nematic phase: solutes

The second-rank orientational order matrix $\boldsymbol{S}_s$ of a solute $s$ of arbitrary symmetry in a N phase is given by the matrix elements

$$S_{s,\gamma\delta} = \frac{\int d\Omega_s \left(\frac{3}{2}\cos\theta_{s,\gamma}\cos\theta_{s,\delta} - \frac{1}{2}\delta_{\gamma\delta}\right) e^{-\frac{H_{N,Ls}(\Omega_s)}{k_B T}}}{\int d\Omega_s e^{-\frac{H_{N,Ls}(\Omega_s)}{k_B T}}} \quad (4)$$

where $H_{N,Ls}(\Omega_s)$ is the anisotropy in the average field felt by the solute and $\Omega_s$ represents the instantaneous orientation of the solute with respect to the director with $\theta_{s,\gamma}$ being the angle between the solute $\gamma$ axis and the director. $\boldsymbol{S}_s$ is symmetric and traceless and, thus in general, contains five independent terms. For liquid-crystal phases that possess axial symmetry (such as the N and SmA phases being considered here), it is convenient to write $H_{N,Ls}(\Omega_s)$ in terms of the anisotropic part of the average axially symmetric liquid-crystal field felt by the solute, $G_{L,ZZ}$, and the anisotropic part of some solute property, $\beta_{s,\gamma\delta}$, that interacts with this field

$$\mathscr{H}_{N,Ls}(\Omega_s) = -\frac{3}{4} G_{L,ZZ} \sum_{\gamma}\sum_{\delta} \cos(\theta_{s,\gamma})\cos(\theta_{s,\delta})\beta_{s,\gamma\delta} \quad (5)$$

We make the average-field approximation that all solutes feel the same liquid-crystal field: the success of this assumption lies in the agreement between theory and experiment that results.

While Eqns (4) and (5) are perfectly general, the nature of $G$ and $\beta$ is not automatically associated with specific intermolecular interaction or interactions. Problems arise with attempts to use these equations in the interpretation of solute order parameters obtained from the dipolar couplings measured by NMR spectra: in essence, it is found that the solute $\beta$ parameters vary with liquid-crystal solvent and with temperature. However, when it is assumed that there are two independent MS interactions that make up the anisotropic solute interactions, it is possible to rationalize solute order parameters in a variety of different N liquid-crystal solvents to about the 5% level.[13] Hence, in this so-called MSMS (double Maier-Saupe) approach, we rewrite Eqn (5) as a sum over two formally identical terms but with distinct liquid-crystal and solute interactions:

$$\mathscr{H}_{N,Ls}(\Omega_s) = -\frac{3}{4}\sum_{i=1}^{i=2} G_{L,ZZ}(i) \sum_{\gamma}\sum_{\delta} \cos(\theta_{s,\gamma})\cos(\theta_{s,\delta})\beta_{s,\gamma\delta}(i) \quad (6)$$

For solutes with sufficient symmetry such that the $\boldsymbol{\beta}(i)$ tensor is diagonal with only two independent components $\beta_{s,zz}(i)$ and $b_s(i)$, this equation can be written

$$\mathscr{H}_{N,Ls}(\Omega_s) = -\frac{3}{4}\sum_{i=1}^{i=2} G_{L,ZZ}(i)\beta_{s,zz}(i) \times \left[\left(\frac{3}{2}\cos^2(\theta_s) - \frac{1}{2}\right) + \frac{b_s(i)}{2}\sin^2(\theta_s)\cos(2\phi_s)\right] \quad (7)$$

where

$$b_s(i) = \frac{\beta_{s,xx}(i) - \beta_{s,yy}(i)}{\beta_{s,zz}(i)} \quad (8)$$

and where $\theta_s$ and $\phi_s$ are the polar and azimuthal angles between the solute and the director.

Two problems with this approach are as follows: (i) there is no unambiguous way of dividing interactions between the two possibilities, and (ii) only $G\beta$ products appear, and thus, for two independent MS mechanisms, there are four degrees of freedom. For the results presented later (shown in Table 1), we fix two of the degrees of freedom by setting $G_1 = 1$ and $G_2 = 0$ for a N phase consisting of 55 wt.% Merck ZLI1132 (1132) and 45 wt.% *p*-ethoxybenzylidene-*p*′-*n*-butylaniline (EBBA) at 298 K. In this particular 'magic' mixture (MM), molecular deuterium feels zero electric field gradient; this observation has been used to fit solute order parameters measured in this liquid-crystal solvent to models for $G\beta$ consisting of short-range intermolecular interactions that depend only on solute size and shape to about the 10% level.[6] Hence, we associate interaction 1 with size-and-shape interactions and interaction 2 with longer-range anisotropic interactions, such as that between the solute polarizability and the solvent mean square electric field or between the solute quadrupole and the solvent mean electric-field gradient. It should be noted that it is assumed that all solutes feel the same $G_1$ and $G_2$ fields in a given liquid crystal at a given temperature; it is the different magnitudes of these two interactions that vary with liquid crystal and with temperature that allow this model to rationalize results for a variety of solutes in a host of liquid-crystal solvents.[13]

**Table 1.** Maier–Saupe solute parameters from Weber *et al.*[22]

| | Solute property ($\beta_{s,\gamma\gamma}(i)$) | |
|---|---|---|
| Solute tensor component | $MS_1$ | $MS_2$ |
| $tcb_{zz}$ | −0.990(13) | −0.207(17) |
| $pdcb_{yy}$ | −0.024(9) | 0.229(13) |
| $pdcb_{zz}$ | −0.951(11) | −0.236(16) |
| $mdcb_{yy}$ | 0.669(6) | 0.079(8) |
| $mdcb_{zz}$ | −0.933(10) | −0.266(14) |
| $odcb_{yy}$ | 0.333(7) | 0.156(9) |
| $odcb_{zz}$ | −0.927(10) | −0.285(13) |
| $fur_{yy}$ | 0.331(6) | 0.227(8) |
| $fur_{zz}$ | −0.529(8) | −0.246(10) |
| $thi_{yy}$ | 0.246(6) | 0.185(8) |
| $thi_{zz}$ | −0.570(8) | −0.262(10) |
| $hex_{zz}$ | 1.066(6) | 0.210(8) |
| $phac_{yy}$ | −0.033(8) | 0.023(11) |
| $phac_{zz}$ | −0.949(12) | −0.359(14) |
| $dcnb_{yy}$ | 0.393(7) | 0.187(11) |
| $dcnb_{zz}$ | −1.126(12) | −0.215(17) |
| $pbbn_{yy}$ | −0.204(10) | 0.190(16) |
| $pbbn_{zz}$ | −1.019(12) | −0.235(19) |
| $clpro_{yy}$ | 0.028(6) | 0.056(8) |
| $clpro_{zz}$ | −0.035(6) | −0.002(8) |
| $fb_{yy}$ | 0.259(8) | 0.207(9) |
| $fb_{zz}$ | −0.751(11) | −0.272(12) |

tcb, 1,3,5-trichlorobenzene; pdcb, 1,4-dichorobenzene; mdcb, 1,3-dichlorobenzene; odcb, 1,2-dichlorobenzene; fur, furan; thi, thiophene; hex, 2,4-hexadiyne; phac, phenylacetylene; dcnb, 1,2-dicyanobenzene; pbbn, para-bromobenzonitrile; clpro, 2,2-dichloropropane; fb, fluorobenzene.

### Smectic A phase: solutes

Upon cooling, some N phases undergo a phase transition to an SmA phase. Such systems are useful for investigating the SmA phase if it can be assumed that the N potential [e.g. Eqn (2)] can be extrapolated into the SmA phase, i.e. be used to give values for $\mathscr{H}_{N,L}(\boldsymbol{\theta}_L)$ in Eqn (3).

In the present work, we are interested in solutes and thus write the SmA potential

$$\mathscr{H}_{SmA,Ls}(\boldsymbol{\Omega}_s, Z) = \mathscr{H}_{N,Ls}(\boldsymbol{\Omega}_s)\left[1+\kappa'_L\cos\left(\frac{2\pi Z}{d}\right)\right] - \tau'_{Ls}\cos\left(\frac{2\pi Z}{d}\right) \quad (9)$$

The orientational order parameters in the SmA phase are given by

$$S_{s,\gamma\gamma} = \frac{\int d\boldsymbol{\Omega}_s \int_0^d \left(\frac{3}{2}\cos^2(\theta_{s,\gamma}) - \frac{1}{2}\right) e^{-\frac{\mathscr{H}_{SmA,Ls}(\boldsymbol{\Omega}_s,Z)}{k_B T}} dZ}{\int d\boldsymbol{\Omega}_s \int_0^d e^{-\frac{\mathscr{H}_{SmA,Ls}(\boldsymbol{\Omega}_s,Z)}{k_B T}} dZ} \quad (10)$$

and the positional order parameter by

$$\tau_{Ls} = \frac{\int d\boldsymbol{\Omega}_s \int_0^d \cos\left(\frac{2\pi Z}{d}\right) e^{-\frac{\mathscr{H}_{SmA,Ls}(\boldsymbol{\Omega}_s,Z)}{k_B T}} dZ}{\int d\boldsymbol{\Omega}_s \int_0^d e^{-\frac{\mathscr{H}_{SmA,Ls}(\boldsymbol{\Omega}_s,Z)}{k_B T}} dZ} \quad (11)$$

## Determining SmA Parameters $\tau'$ and $\kappa'$

The body of experimental work that is reviewed later generally involved the study of several solutes that were usually codissolved in the same NMR tube in the liquid crystal 8CB, 8OCB or a mixture of 8OCB and 6OCB. These liquid crystals (except pure 6OCB) exhibit both N and SmA phases. The codissolving of solutes was used in order to ensure that all solutes experience precisely identical environments, hence avoiding problems that arise when trying to compare results from different sample tubes that have differing overall composition.

Figure 1 displays an example NMR spectrum obtained from one of the samples.[14] The complicated NMR spectra (a superposition of spectra from all five solutes; Figure 1) that are then obtained are readily analyzed using a covariance matrix adaptation evolutionary strategy (CMA-ES).[15,16] To obtain the spectral parameters with the CMA-ES, one has to first choose reasonable upper and lower limits for each parameter (called a gene), which defines the search space. A complete set of these genes represents a calculated spectrum (called a chromosome), and a population of these is initially spread out randomly across the search space. To evaluate the goodness of each member of the population, a fitness function is used, which gives a measure of the extent to which calculated spectra overlap with the experimental one. The overlap is maximum at the global minimum of the error surface, which has a large number of local minima. To reach the global minimum and escape local minima, the chromosomes with the best fitness function are used to create the offspring of subsequent generations in a mutative step-size fashion. The trajectory through parameter space of each generation is influenced by the vectors of previous ones. When such a strategy is used, automatic and simultaneous solutions of multiple solute spectra are obtained.[17]

For the sake of clarity, we shall concentrate our discussion on the solute pdcb only. Experimental results that demonstrate the effect of the SmA-phase layering are presented in Figure 2 (left) where it is seen that the anisotropy $R = (S_{xx} - S_{yy})/S_{zz}$ of the order matrix for pdcb in 8CB changes abruptly at the N–SmA phase transition. The transition is barely detectable directly from order-parameter values themselves, but the change in slope of the asymmetry is clear and indicates that the $S_{s,ii}$ values could be used to obtain information about the SmA potential.[18]

To proceed, we fit the two pdcb solute order parameters determined at each temperature to Eqns (4) and (7) ($i = 1$ term only) and determine the two parameters of the N potential, $b_s$ and $\beta_{s,xx}$, plotting one *versus* the other in Figure 2. We note the linear dependence in the N phase and assume that the line through the N points can be extrapolated into the SmA phase in order to give the N potential in the SmA phase. We then use Eqns (9) and (10) to fit the difference between the values determined with $H_{N,Ls}$ and the extrapolated values to find the fitted values of $\tau'_{Ls}$ and $\kappa'_L$ for the SmA phase. We assume that $\kappa'_L$ is positive, which is consistent with the N ordering being maximum near the core (centre) of a smectic layer.[19] In the paper, the results were fitted to an assumed constant $\kappa'_{Ls}$ and a temperature-dependent $\tau'_{Ls} = \tau'_{0,s}(1 + \tau'_1 T/300\ \mathrm{K})$. The results for a second solute [fluorobenzene (fb)] used the same value of $\tau'_1$ and gave almost equal values for $\kappa'_{Ls}$ but very different values for $\tau'_{0,s}$. These results are quite encouraging as the N–smectic coupling $\kappa'_{Ls}$ is expected to be a liquid-crystal property ($\kappa'_L$, independent of solute $s$), whereas differing $\tau'_{0,s}$ values for different solutes indicates different solute positional preferences within the smectic layers. One problem with these results is that the values obtained for $\kappa'_L$ are close to 1. Examination of Eqn (9) shows that the value $\kappa'_L = 1$ would result in the N potential $\mathscr{H}_{N,Ls}(\boldsymbol{\Omega}_s)[1+\kappa'_L\cos\left(\frac{2\pi Z}{d}\right)]$ being zero at $Z = d/2$, hence giving an isotropic region at the smectic interlayer. Such an isotropic region

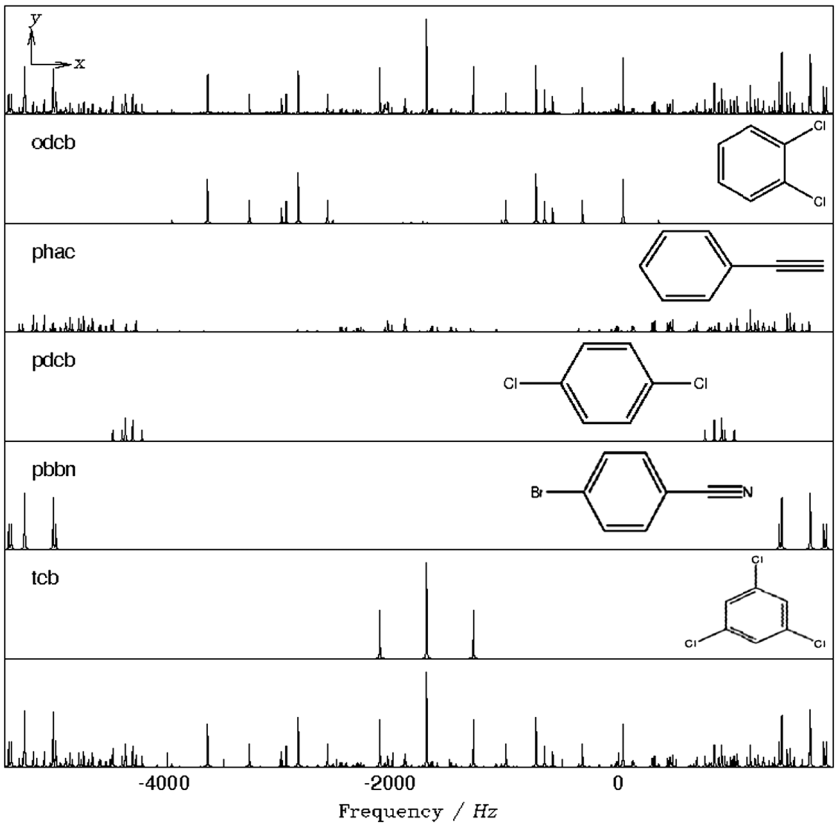


**Figure 1.** $^1$H NMR spectra of five codissolved solutes in a sample of 27 wt.% 6OCB/73 wt.% 8OCB in the N phase (sample 4 of Burnell *et al.*[14]) at 339.5 K. The upper plot is of the experimental 400 MHz NMR spectrum while the bottom plot is a sum of the calculated spectra. The calculated spectra of the solutes from top to bottom are *ortho*-dichlorobenzene (odcb), phenylacetylene (phac), *para*-dichlorobenzene (pdcb), *para*-bromobenzonitrile (pbbn) and 1,3,5-trichlorobenzene (tcb) with the molecule-fixed coordinate system being found in the top left of the figure. Reproduced with permission from Burnell *et al.*[14]

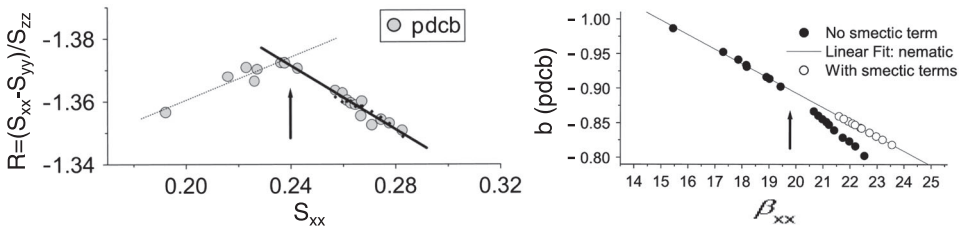


**Figure 2.** Left: An order-matrix 'asymmetry' parameter $R = (S_{xx} - S_{yy})/S_{zz}$ is plotted against $S_{xx}$ and is sensitive to the dissimilar environments experienced by solutes in the nematic and smectic-A phases of 8CB. There is a change in slope on either side of the phase transition (denoted by the arrow). The gray line is a linear fit to the nematic-phase points. The solid black line plots asymmetry parameters calculated from a fit to smectic order. This panel is a modified version of part of Fig 1(b) of Yethiraj *et al.*,[18] reprinted with permission. Right: The asymmetry $b$ plotted against $\beta_{xx}$ (solid symbols) exhibits a linear dependence in the nematic phase and is roughly linear but with different slope in the smectic-A phase. The nematic/smectic-A phase lies to the left/right of the arrow, which denotes the phase-transition point. We introduce a *smecticity* and a nematic–smectic-A coupling term into the intermolecular potential [Eqn (9)] and refit the results (open symbols) requiring $b$ in the smectic-A phase to fall on the extrapolation to the linear fit in the nematic phase. Both pdcb and fluorobenzene results are simultaneously fit in the smectic phase to five parameters (see text) representing the strengths of the coupling and smecticity. This panel is a modified version of part of Figure 2 of Yethiraj *et al.*[18] (the original typographical sign error in $b$ is corrected), reprinted with permission from Yethiraj *et al.*[18]

is unlikely, even in the hydrocarbon region of smectic layers.[20] More details can be found in the study of Yethiraj *et al.*[18]

Next, we examine the results for pdcb with more extensive results for 8CB and also in a different liquid-crystal solvent, 4-*n*-octyloxy-4′-cyanobiphenyl (8OCB), which forms a higher-temperature N phase and a lower-temperature SmA phase.[20] This time, the plot of $R$ *versus* $S_{xx}$ (shown for 8OCB only in Figure 3) is again linear in the N phase but shows curvature and goes through a maximum in the SmA phase. However, when the N parameters are calculated and plotted as in Figure 2, they are

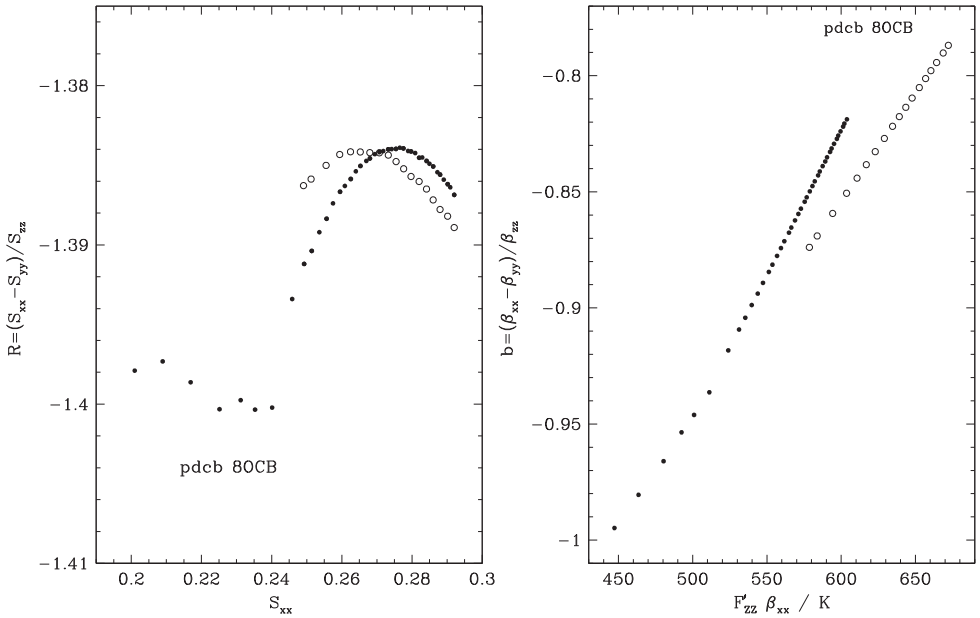


**Figure 3.** Left: Order parameter ratio $R = \frac{S_{xx}-S_{yy}}{S_{zz}}$ *versus* $S_{xx}$ for pdcb in 8OCB. Filled points are the experimental values, and open circles are the values calculated from a fit to the three solutes 1,2-dichlorobenzene (odcb), 1,3-dichlorobenzene (mdcb) and pdcb in the same liquid crystal; $\kappa'_{8OCB} = 0.38$ was varied but kept equal for all solutes (pdcb, mdcb and odcb) in the fitting. The value of $\tau''$ is fitted for each solute in each liquid crystal and is scaled by $F_{ZZ}\beta_{zz}$ to give $\tau' = \tau'' F_{ZZ}\beta_{zz}$ for each experiment. The values obtained for $\tau''_{pdcb}$ is 0.298. Nematic-phase points are to the left, and smectic A phase points to the right. Right: The asymmetry in the energy $b$ plotted *versus* $F'_{ZZ}\beta_{xx}$ where $F'_{ZZ} = F_{ZZ}/k_B$. The filled circles are the exact fitting of the solute orientational order parameters to the two independent $\beta_{ii}$ energy parameters of Eqns (7) and (8) (with only one term in the sum). The intercepts and slopes of the straight line drawn through the nematic points are reported in Table 2 of Yethiraj *et al*.[20] The open circles are the $b$ and $F'_{ZZ}\beta_{xx}$ values from the fit to the smectic potential, Eqn (9). As required by the extrapolation procedure used to obtain the nematic part of the potential in the smectic A phase, these points all fall on the nematic line. The points for the nematic phase are to the left, and those for the smectic A phase to the right. Reproduced with permission from parts of Figures 3 and 4 of Yethiraj *et al*.[20]

again found linear with differing slopes in both the N and SmA phases (see right panel of Figure 3 for 8OCB). Again, the difference between extrapolated and calculated values allows determination of the SmA-phase parameters. This time, a more reasonable value for $\kappa'_L = 0.4$ is obtained when the value of $\tau'_{Ls}$ is scaled to the N potential, perhaps a more reasonable choice than the linear scaling with the temperature used earlier. From Figure 3 (left side), it is seen that the fit to the order parameter asymmetry $R$ is not perfect but the general trend is achieved.

### Solutes in a liquid crystal with a reentrant-nematic (RN) phase

Some liquid crystals, e.g. mixtures of 4-*n*-hexyloxy-4′-cyanobiphenyl (6OCB) and 8OCB, exhibit the interesting phenomenon of forming a high-temperature N phase and a low-temperature RN phase, which is separated from the high-temperature phase by an SmA phase. Figure 4 (left) presents the results in terms of the two independent components of the order parameter matrix, plotted as $R$ *versus* $S_{zz}$, for the three solutes pdcb (same solute as in Figures 2 and 3), mdcb and odcb (larger absolute values of $S_{zz}$ are lower temperatures). The results show curvature with pdcb exhibiting an interesting S-shaped curve. The N energy parameters $F'_{ZZ}\beta_{xx}$ and $b$ calculated from these order parameters are presented in Figure 4 (right), with the higher-temperature N-phase values to the left. For pdcb and mdcb, the N-phase points form a linear plot, but the odcb values exhibit curvature. In this case, a curve that goes through both N and RN points is used in order to extrapolate the N potential into the SmA phase. For mdcb, but not for pdcb, the linear extrapolation of the N points goes through the RN points.[21]

### Nematic phase: solutes and the MSMS potential

Several problems remain with the previous analysis of the smectic potential. The extrapolation of N-phase values is particularly difficult with the curvature apparent in some of the graphs. Also, from Figures 2–4, it can be seen that the previous treatments involve changes with temperature or liquid-crystal solvent in the solute asymmetry parameter $b_s$ for all solutes. As $b_s$ is some solute property, such dramatic changes in the asymmetry are unexpected. While breakdown of the simple MS theory might account for the changes, the overwhelming suggestion is that more than one anisotropic intermolecular mechanism is at play. Past experience indicates that two mechanisms are sufficient to explain solute order parameters in N solvents using Eqn (7).[13] To check out and use this idea for the N potential in SmA phases, a study of 12 solutes in two different liquid-crystal solvents was used.

As mentioned earlier, a problem now arises because in Eqn (7) $G$ and $\beta$ always appear as products with the same angular dependency. Thus, for two independent MS mechanisms, there are four degrees of freedom, and hence, four values must be fixed in order to do a least squares fit to the experimental order parameters. As mentioned earlier, we set $G_1 = 1$ and $G_2 = 0$ for MM, which means that we associate interaction 1 with short-range size-and-shape interactions and interaction 2 with longer-range interactions. In order to provide a scale for this second interaction,

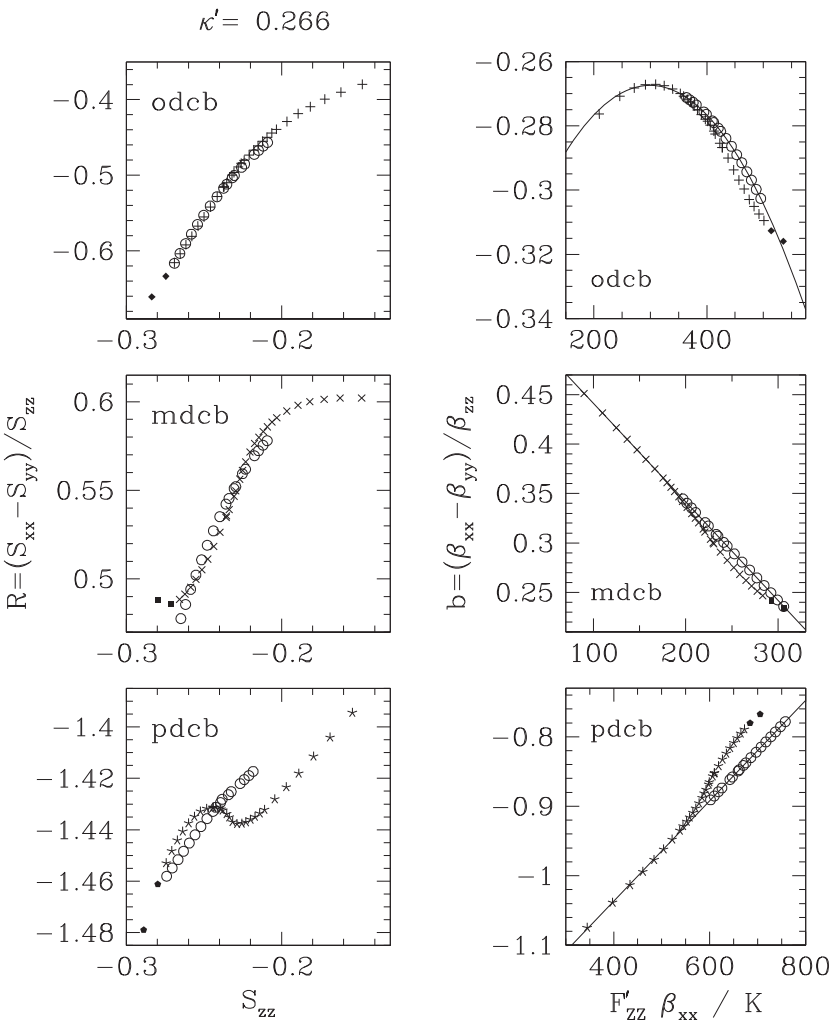


**Figure 4.** Asymmetry parameters $R$ and $b$ for solutes in the liquid-crystal mixture 72 wt.% 8OCB/28 wt.% 6OCB. Left: Order parameter ratio $R = \frac{S_{xx}-S_{yy}}{S_{zz}}$ *versus* $S_{zz}$ (skeletal points). Open circles are values calculated from a fit to the three solutes odcb, mdcb and pdcb in the SmA phase of the liquid-crystal mixture. $\kappa'_L = 0.266$ was varied but kept equal for all solutes at all temperatures. A separate value of $\tau''$ is fitted for each solute and is scaled by $F_{ZZ}\beta_{zz}$ to give $\tau' = \tau'' F_{ZZ}\beta_{zz}$ for each experiment. Nematic-phase points are to the right, and smectic A phase points to the left with the two filled points to the far left being from the RN phase. Right: Asymmetry in the energy $b$ plotted *versus* $F'_{ZZ}\beta_{xx}$ where $F'_{ZZ} = F_{ZZ}/k_B$. The experimental $S_{ii}$ are used for the exact fitting of the solute orientational order parameters to the two independent $\beta_{ii}$ energy parameters $b$ and $\beta_{xx}$ (skeletal points). The intercepts and slopes of the straight lines drawn through the nematic skeletal points for mdcb and pdcb are reported by Yethiraj *et al.*,[21] while odcb has a curved fit to the nematic points as detailed in Yethiraj *et al.*[21] The open circles are the $b$ and $F'_{ZZ}\beta_{xx}$ values from the fit to the smectic potential, Eqn (9). The points for the nematic phase are to the left, and those for the smectic A phase to the right, with the two filled points to the far right being from the RN phase. Reproduced with permission from parts of Figures 1 and 2 of Yethiraj *et al.*[21]

we arbitrarily set $G_2 = 1$ for 1132. These three arbitrary assignments impose no restrictions on the problem. However, we must fix one further value. We do not wish to give any physical meaning to the second mechanism and hence do not wish to fix further values of $G_2$. Hence, as was performed in the original MSMS paper,[13] we set equal $G_1$ values for 1132 and EBBA: in other words, we assume that size-and-shape interactions are equal in these two liquid-crystal solvents. Note that these four assignments are completely arbitrary and are chosen to give a qualitative significance to the $G$ (and hence, the $\beta$) parameters.

The solute $\beta$ parameters are now obtained from a least-squares fit [using the potential of Eqn (7) in Eqn (4)] to the orientational order parameters for the 12 solutes at a single temperature in liquid crystals 1132, MM and EBBA and at three different temperatures spanning the N ranges of 8CB and 8OCB.[22] The values obtained are given in Table 1. Values for solutes that were included in the original study[13] do not differ significantly from the values found there.

Now that we have the solute $\beta$ parameters, we can use them in a least-squares fit to the solute order parameters to find $G_1$ and $G_2$ values for 8CB and for 8OCB at each experimental temperature in both the N and SmA phases – the values obtained are displayed as the open circles in Figure 5 where the quality of fit is also indicated by the RMS (root mean square) difference between experimental and recalculated order parameters. The excellent fit (low RMS) found for the N phase is a strong indication that the MSMS theory applies, and the larger RMS differences for the SmA phase indicate the need for an additional term in the potential.

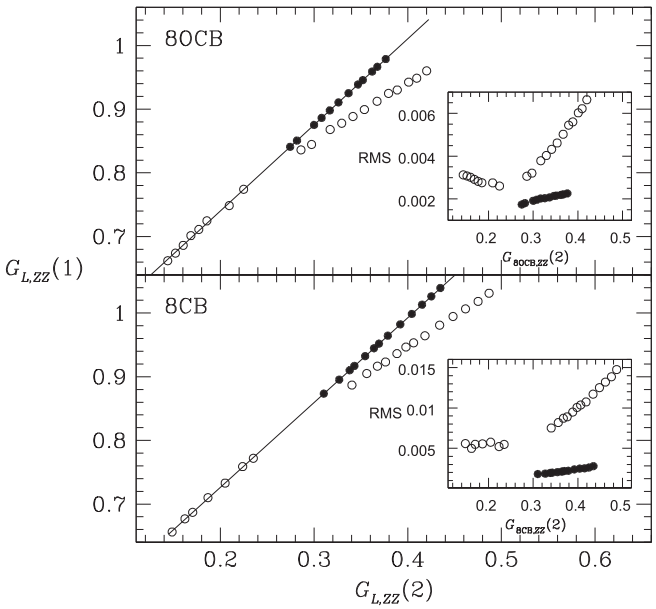


**Figure 5.** $G_{L,ZZ}(1)$ is plotted against $G_{L,ZZ}(2)$ where the filled points signify the use of the smectic interaction potential Eqn (13) and the open points are obtained with the nematic potential Eqn (7) only. The seven (8CB) or eight (8OCB) points closest to the origin are from measurements in the nematic phase while the rest are in the smectic phase. *Inset*: The RMS of fits to either potential in both phases are plotted against $G_{L,ZZ}(2)$. Reproduced with permission from Weber *et al.*[22]

For comparison with the earlier studies, it is convenient to define a $\beta$ asymmetry that includes the two interactions. We note that Eqn (7) contains the term $[G_{L,ZZ}(1)(\beta_{s,xx}(1)-\beta_{s,yy}(1))+G_{L,ZZ}(2)(\beta_{s,xx}(2)-\beta_{s,yy}(2))]$. Hence, we can express the asymmetry in the $\beta$ parameters by

$$b_{s,\,\mathrm{MSMS}}=\frac{\frac{G_{L,ZZ}(1)}{G_{L,ZZ}(2)}(\beta_{s,xx}(1)-\beta_{s,yy}(1))+(\beta_{s,xx}(2)-\beta_{s,yy}(2))}{\frac{G_{L,ZZ}(1)}{G_{L,ZZ}(2)}\beta_{s,zz}(1)+\beta_{s,zz}(2)} \quad (12)$$

Figure 6 uses open symbols and $G$ values from the N potential of Eqn (7) to display this asymmetry (open symbols) for solute pdcb as a function of temperature.

### Smectic A phase: solutes and the MSMS-KM potential

To deal with the SmA phase, we add the KM SmA terms to the N-phase MSMS potential, Eqn (7):

$$\mathscr{H}_{SmA,Ls}(\mathbf{\Omega}_s,Z)=-\frac{3}{4}\sum_{i=1}^{i=2}G_{L,ZZ}(i)\beta_{s,zz}(i)\left[1+\kappa'_L(i)\cos\left(\frac{2\pi Z}{d}\right)\right]\times\left[\left(\frac{3}{2}\cos^2(\theta_s)-\frac{1}{2}\right)+\frac{b_s(i)}{2}\sin^2(\theta_s)\cos(2\phi_s)\right]-\tau'_{Ls}\cos\left(\frac{2\pi Z}{d}\right) \quad (13)$$

We now wish to use this equation to fit the experimental orientational order parameters[22] in the SmA phases using Eqn (10). If in the fitting we vary both $G$ parameters and all SmA parameters ($\tau'_{Ls}$, $\kappa'_L(1)$ and $\kappa'_L(2)$), we do not obtain convergence. However, we note in Figure 5 that a plot of $G(1)$ *versus* $G(2)$ is linear in the N phase. Thus, similar to most previous treatments, we assume that this linear relationship can be extrapolated into the SmA phase (solid lines in Figure 5). Fitting to the order parameters measured in the SmA phase now gives values for $G(2)$, $\tau'_{Ls}$, $\kappa'_L(1)$ and $\kappa'_L(2)$ [and $G(1)$ from the value of $G(2)$ and the line in Figure 5]. The $b_{\mathrm{pdcb,MSMS}}$ calculated from these $G$ values are displayed as the solid points in Figure 6. As was the case for the $b_s$ values calculated earlier, the general trend is for the molecular asymmetry to decrease in the SmA phase compared with the values from the N-phase extrapolations.

In order to gain insight into the modulation of the N potential in the smectic layers, we plot in Figure 7 the modulation of the two N mechanisms [the $i=1$ and $i=2$ terms of the sum in Eqn (13), labeled $\mathscr{H}_N^{\mathrm{mod}}(i)$] and their sum ($\mathscr{H}_N^{\mathrm{tot}}$) for the solute pdcb with each symmetry axis in turn oriented along the director of 8OCB (top) or 8CB (bottom). The $x$ axis coincides with the Cl–Cl direction, $z$ is perpendicular to the benzene ring, and $y$ is perpendicular to $x$ and $z$. The general trends are the same for the two

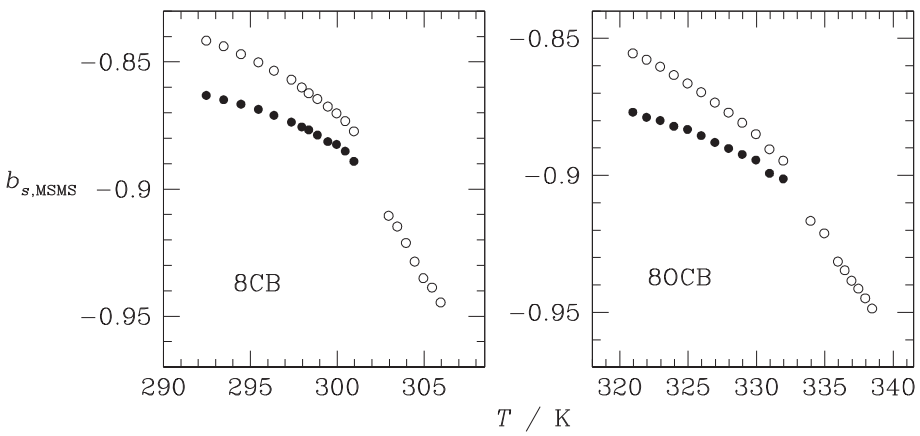


**Figure 6.** $b_{\mathrm{pdcb,MSMS}}$ is plotted against temperature for pdcb in 8OCB and 8CB. Points in the smectic phase are to the left, and those in the nematic to the right. The open circles were obtained using the nematic potential Eqn (7), and the filled circles used the smectic potential Eqn (13). Reproduced with permission from Weber *et al.*[22]

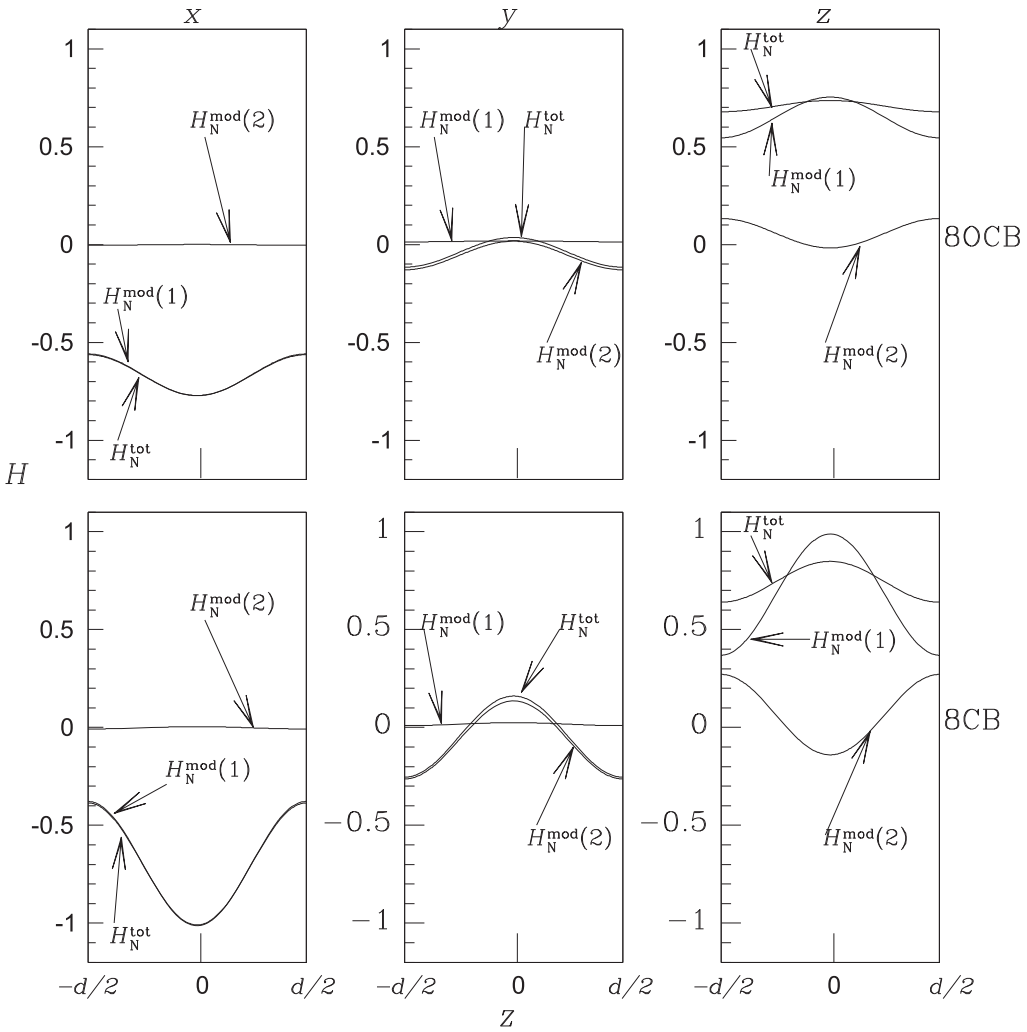


**Figure 7.** The modulation of each nematic mechanism from smectic layering $H_N^{mod}(i)$ and their sum $H_N^{tot}$ in 8CB at 298.0 K and 8OCB at 327.0 K for pdcb where each molecule-fixed axis is, in turn, oriented along the director. The centre of the layer is at the origin. Reproduced with permission from Weber *et al.*[22]

liquid-crystal solvents. With *z* along the director, $\mathscr{H}_N^{mod}(1)$ is positive, consistent with packing arguments against the benzene ring plane being perpendicular to the director. This effect is largest at the layer centre as might be expected for interactions between the core region of the liquid-crystal molecules and the perpendicular orientation of the solute benzene ring; these interactions are lesser when involving the liquid-crystal interlayer (hydrocarbon tail) region. The opposite holds when the pdcb *x* axis (Cl–Cl direction) is along the director, the lower energy (particularly at the layer centre) favoring this orientation. This makes sense from shape arguments as this region contains the aromatic core of the liquid-crystal molecules, which would be expected to exert more of an orientational influence than that of the hydrocarbon tail region.

The second mechanism is consistent with interactions between molecular quadrupoles. For example, the interaction between unlike quadrupoles is negative, giving low energy at the layer centre when the pdcb *z* axis is aligned along the director (i.e. for perpendicular adjacent benzene rings).

## An alternative way of extrapolating the N potential into the SmA phase

One overriding problem with all the previous studies is the need to define the N potential in the SmA phase. There is no direct link between the measured solute orientational order parameters and this N potential, so we have relied on some form of extrapolation of N parameters from values in the N phase.

As indicated earlier, the phase diagram for mixtures of the liquid crystals 6OCB and 8OCB shows an interesting region of concentrations for which both N (at higher *T*) and RN (at lower *T*) phases exist, these phases being separated at intermediate temperatures by a SmA phase. This suggests the extrapolation with composition of N parameters from the N into the SmA phase. Hence, the five solutes of Figure 1 were codissolved in various mixtures of 6OCB and 8OCB and spectra obtained as a function of temperature and composition.[14] Two of the samples have a small temperature region of SmA phase between N and RN phases, and two are entirely in the N phase.

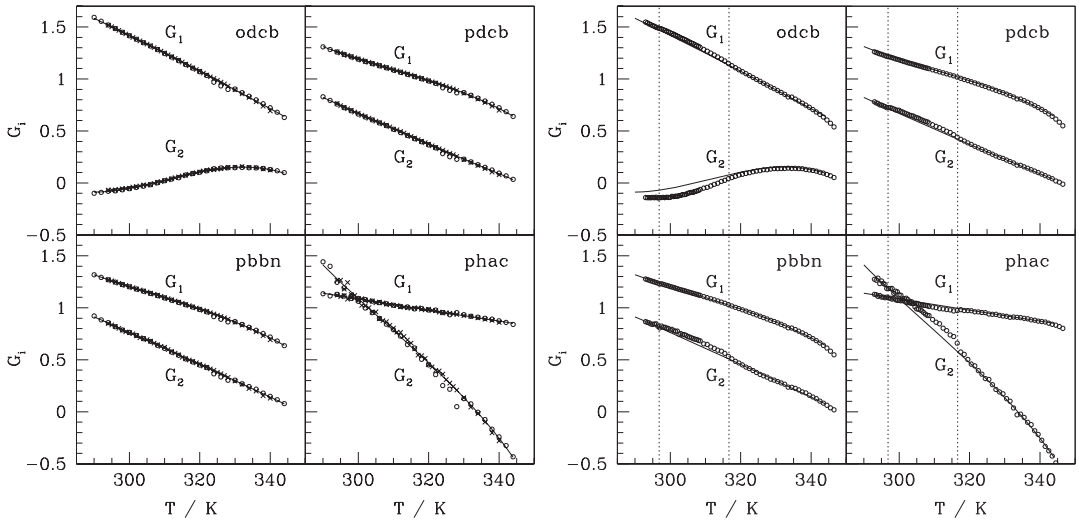


**Figure 8.** Left panels: $G_{L,ZZ}(1)$ and $G_{L,ZZ}(2)$ derived with the nematic potential only, Eqn (7), in samples 7 (30.1 wt.% 6OCB) and 8 (31.8 wt.% 6OCB). Lines denote polynomial fits to the $G_{L,ZZ}(i)$ values. Sample 7: ∘ and sample 8: ×. Right panels: The points are $G_{L,ZZ}(1)$ and $G_{L,ZZ}(2)$ values from fits of the nematic potential only, Eqn (7), to orientational order parameters for sample 4 (27.0 wt.% 6OCB) *versus T*. The solid lines are the polynomial fits in the left panels to $G_{L,ZZ}(1)$ and $G_{L,ZZ}(2)$ values determined for fits of the nematic potential to samples 7 and 8. Reproduced with permission from parts of Figures 3 and 4 of Burnell *et al*.[14]

The dipolar couplings obtained in the analysis are used to obtain the molecular order parameters, and these in turn [from a fit to the MSMS N potential of Eqn (7) with the solute $\beta$ parameters in Table 1] are used to obtain $G_{L,ZZ}(1)$ and $G_{L,ZZ}(2)$ values for each solute at each temperature for the two N-phase samples, as displayed in Figure 8 (left side). Of course, the $G_{L,ZZ}(i)$ are supposed to be liquid-crystal parameters and hence independent of solute. Here, however, we wish to extrapolate values as a function of composition into the SmA phase and wish to do this as accurately as possible. Hence, we allow a solute dependence of $G_{L,ZZ}(i)$ and perform separate extrapolations for each solute.

The $G_{L,ZZ}(i)$ values for the N phase of two of the samples (sample 7, 30.1 wt.% 6OCB, and sample 8, 31.8 wt.% 6OCB)[14] are fitted to a polynomial [see lines in Figure 8 (left)]. These lines are included in the right side of Figure 8 for sample 4 of Burnell *et al*.[14] that does exhibit an SmA phase. The points for sample 4 lie on the lines for the higher-temperature N-phase points, justifying the proposed extrapolation of $G_{L,ZZ}(i)$ parameters from the N into the SmA phase. Thus, the differences between the lines and the $G_{L,ZZ}(i)$ values obtained in the fit to the N potential are taken to result from the smecticity. A least-squares fit using these differences gives values for $\kappa_L'(1)$, $\kappa_L'(2)$, and $\tau_s'$ for each solute at each temperature within the SmA phase. As earlier, the $\kappa_L'(i)$ are assumed to be a liquid-crystal property. Here, we are essentially extrapolating the N-phase $G_{L,ZZ}(i)$ values as a function of concentration.

In Figure 9 (bottom two panels), we present a plot of $G_{L,ZZ}(1)$ *versus* $G_{L,ZZ}(2)$ for odcb and pdcb in sample 4 that exhibits N, SmA and RN phases. These plots have distinct curvature, unlike the results reported earlier in Figure 5 for 8CB and 8OCB for which the plots had one linear region in the N phase and a separate linear region in the SmA phase. Of course, these 8CB and 8OCB plots are from a fit to results for several solutes. The curvature in the plots for separate solutes in the 6OCB/8OCB mixture can be thought of as showing pre-transitional behaviour as the sample becomes closer in temperature to the SmA phase. The change of curvature for odcb in the N phase as we approach the SmA phase and the reverse for the RN phase is particularly noteworthy.

The flexible solute *n*-butane was also investigated in a 6OCB/8OCB mixture that exhibits N, SmA and RN phases.[9] The results are summarized in a separate paper[10] in this journal volume.

## Liquid-crystal mixture exhibiting two nematic phases, N and $N_x$: solutes

Figure 9 (top three panels) incorporates plots from a study of a mixture of 39 wt.% 4-*n*-pentyl-4′-cyanobiphenyl (5CB) in $\alpha,\omega$-bis(4-4′-cyanobiphenyl)nonane (CBC9CB) that exhibits two different N phases as a function of temperature.[23] The lower-temperature phase, called the $N_x$ phase (indicating uncertainty about its structure), or more recently, the $N_{tb}$ phase (tb standing for the proposed twist-bend nature of this phase), is proposed to consist of a mixture of right-handed and left-handed helices. The interesting point is that the pre-transitional behaviour displayed by the three solutes employed in the study is reminiscent of especially the result for odcb in a sample that had an RN phase (see section on *An Alternative Way of Extrapolating the N Potential into the SmA Phase*). This pre-translational behaviour involves a marked change in $G_{L,ZZ}(2)$. In the plots, a separate $G_{L,ZZ}(2)$ is found for each solute; however, precisely the same trend is found if all three solutes are forced to have the same $G_{L,ZZ}(1)$ and $G_{L,ZZ}(2)$ values – the only effect being a slightly higher RMS difference for the fitting. In both cases, a change in $G_{L,ZZ}(2)$ is observed in the pre-transitional region, this change being associated with some long-range electrostatic interaction, such as that involving molecular quadrupoles or polarizabilities. These results suggest the importance of such interactions in the formation of the smectic and $N_x$ phases.

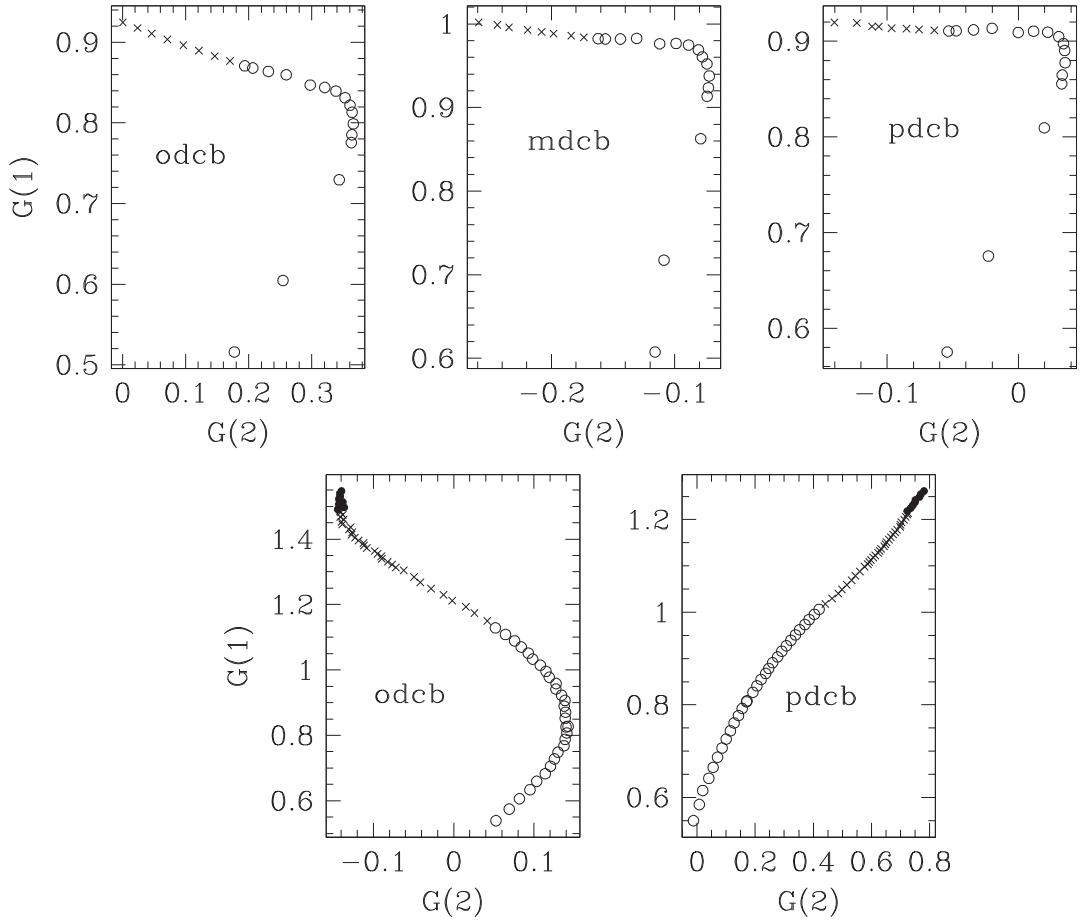


**Figure 9.** Nematic potential parameters $G_{L,ZZ}(1)$ *versus* $G_{L,ZZ}(2)$ for the solutes odcb, mdcb and pdcb in the CBC9CB/5CB mixture that exhibits N (open circles) and $N_x$ (crosses) phases (top) and of odcb and pdcb in the 6OCB/8OCB mixture that exhibits N (open circles), SmA (crosses) and RN (filled circles) phases (bottom). Reproduced with permission from Dong *et al.*[23]

**Table 2.** Smectic A solute $\tau$ order parameters

| Calculation | Liquid crystal | *T* range | $\tau_{pdcb}$ | $\kappa'$ or $\kappa'_1, \kappa'_2$ |
|---|---|---|---|---|
| MS[18] | 8CB | 294 to 301 | −0.33 to −0.29 | 0.9 |
| MS[20] | 8CB | 291 to 300 | −0.25 to −0.21 | 0.41 |
| MS[20] | 8OCB[a] | 316 to 333 | −0.23 to −0.19 | 0.38 |
| MS[21] | 28 wt.% 6OCB in 8OCB | 300 to 327 | −0.4 to −0.3 | 0.27 |
| MSMS[22] | 8CB | 292 to 301 | −0.12 to −0.05 | 0.45, −3.15 |
| MSMS[22] | 8OCB | 321 to 332 | −0.2 to −0.1 | 0.16, −1.37 |
| MSMS[14] | 27.0 wt.% 6OCB in 8OCB[b] | 297 to 316 | −0.010 to +0.003 | 0.28, −1.3 |

[a]Note that the labels odcb and pdcb in the right-hand side of Figure 6 of Yethiraj *et al.*[20] should be interchanged.
[b]Sample 4 of Burnell *et al.*[14]

## Smectic Parameters

One of the main objectives of this sort of work is to obtain values for the smectic order parameter $\tau_s$ [Eqn (11)] and the coupling prefactor $\kappa'$. Values for pdcb from the different approaches discussed earlier are tabulated in Table 2. As can be seen, all $\tau_{pdcb}$ are negative, consistent with pdcb preferring the interlayer (hydrocarbon chain) region of the smectic layers. However, the values become progressively smaller (in absolute value) as we do more sophisticated extrapolations of the N potential. When the same analysis is used for both liquid crystals, we find essentially equal solute $\tau$ values for pdcb in both 8CB and 8OCB. However, there are large differences with the method of analysis. Values for the 6OCB/8OCB sample that forms an RN phase demonstrate a

dramatic difference with the analysis method. However, the earlier analysis here was fraught with difficulties imposed by the curvature in the points used for the extrapolation, and indeed for pdcb, the extrapolation through the SmA phase did not go through the RN points.

Except for the initial paper,[18] the values in Table 2 of $\kappa_L'$ [and of $\kappa_L'(1)$ when two N mechanisms are being considered] are in the range of 0.2 to 0.5, depending on extrapolation method. This indicates that, as expected, there is a much larger N ordering potential in the middle of a smectic layer than there is in the interlayer (hydrocarbon tail) region. The interesting result is that $\kappa_L'(2)$ (for the second mechanism) is negative with absolute value greater than 1. Thus, for the long-range electrostatic interaction, the N potential in Eqn (13) is negative in the centre of the smectic layer and changes sign as we go through the layer. Hence, mechanism 2 has the greatest N ordering in the hydrocarbon tail region, with ordering in the layer centre opposing that involved with shape interactions (mechanism 1).

The group at Calabria has proposed an alternative methodology to obtain the solute's positional–orientational distribution function and the solvent's positional order parameter by combining NMR with statistical thermodynamic density functional theory.[24,25] In essence, a knowledge of the solute–solvent interaction is adopted and a certain positional–orientational distribution function for the solvent is assumed. In this connection, these authors have recently reported on pdcb as one of the solutes dissolved in 8OCB.[26] The solvent $\tau$ order parameter of 8OCB was found to be 0.5 at $T/T_{NI} = 0.93$.

## Conclusions

We have presented several different ways of analyzing solute NMR results for samples that have a higher-temperature N phase with a lower-temperature SmA phase in order to obtain information about the smectic phase. In all cases, the main problem has been the description of the N potential within the smectic phase. We have explored several different ways of extrapolating the N parameters into the SmA phase. The important point is whether the different methods yield consistent values of the smectic-phase parameters. Probably, the methods of analysis that employ MSMS-KM theory give the most trustworthy numbers for the smectic prefactor $\tau'$. Hence, $\tau_{pdcb}$ is most likely in the range of $-0.2$ to 0, meaning that this solute is preferentially (slightly) found in the interlayer region of the smectic layers. For the sake of clarity, we concentrated our discussion on the solute pdcb, but similar quantitative statements can be made for other dissolved solutes.

#### Acknowledgement

This work was supported by the Natural Sciences and Engineering Research Council of Canada (NSERC).

## References

[1] S. Chandrasekhar, *Liquid Crystals*, Cambridge University Press, Cambridge, **1992**.
[2] J. W. Emsley, *Nuclear Magnetic Resonance of Liquid Crystals*, vol. C 141, NATO ASI Series, Reidel, Dordrecht, **1985**.
[3] R. Y. Dong, *Nuclear Magnetic Resonance of Liquid Crystals,* 1st edition, Springer-Verlag, New York, **1994**.
[4] W. Maier, A. Saupe, *Z. Naturforsch. A* **1959**, *14*, 882–889.
[5] W. Maier, A. Saupe, *Z. Naturforsch. A* **1960**, *15*, 287–292.
[6] E. E. Burnell, C. A. de Lange, *Chem. Rev. (Washington, D.C.)* **1998**, *98*, 2359–2387, and references therein.
[7] E. E. Burnell, C. A. de Lange, *NMR of Ordered Liquids*, Kluwer Academic Publishers, Dordrecht, The Netherlands, ISBN 1-4020-1343-4, **2003**.
[8] E. E. Burnell, A. C. J. Weber, C. A. de Lange, W. L. Meerts, R. Y. Dong, *J. Chem. Phys.* **2011**, *135*, 234506–234506-10.
[9] A. C. J. Weber, R. Y. Dong, W. L. Meerts, X. Yang, E. E. Burnell, *J. Phys. Chem. A* **2013**, *117*, 9224–9234.
[10] A. C. J. Weber, D. H. J. Chen, *published in this issue,* **2014**.
[11] K. K. Kobayashi, *Mol. Cryst. Liq. Cryst.* **1971**, *13*, 137–148.
[12] W. L. McMillan, *Phys. Rev. A* **1971**, *4*, 1238–1246.
[13] E. E. Burnell, L. C. ter Beek, Z. Sun, *J. Chem. Phys.* **2008**, *128*, 164901–164901-10.
[14] E. E. Burnell, R. Y. Dong, A. C. J. Weber, X. Yang, A. Yethiraji, *Can. J. Chem.* **2011**, *89*, 900–908.
[15] W. L. Meerts, M. Schmitt, *Int. Rev. Phys. Chem.* **2006**, *25*, 353–406.
[16] W. L. Meerts, C. A. de Lange, A. C. J. Weber, E. E. Burnell, *eMagRes* **2013**, *2*, 437–450. DOI: 10.1002/9780470034590.emrstm1309.
[17] A. C. J. Weber, X. Yang, R. Y. Dong, W. L. Meerts, E. E. Burnell, *Chem. Phys. Lett.* **2009**, *476*, 116–119.
[18] A. Yethiraj, Z. Sun, R. Y. Dong, E. E. Burnell, *Chem. Phys. Lett.* **2004**, *398*, 517–521.
[19] G. Cinacchi, *Chem. Phys. Lett.* **2005**, *416*, 238–245.
[20] A. Yethiraj, A. C. J. Weber, R. Y. Dong, E. E. Burnell, *J. Phys. Chem. B.* **2007**, *111*, 1632–1639.
[21] A. Yethiraj, E. E. Burnell, R. Y. Dong, *Chem. Phys. Lett.* **2007**, *441*, 245–249.
[22] A. C. J. Weber, X. Yang, R. Y. Dong, E. E. Burnell, *J. Chem. Phys.* **2010**, *132*, 034503–034503-8.
[23] R. Y. Dong, A. Kohlmeier, M. G. Tamba, G. H. Mehl, E. E. Burnell, *Chem. Phys. Lett.* **2012**, *552*, 44–48.
[24] G. Celebre, G. Cinacchi, G. De Luca, *J. Chem. Phys.* **2008**, *129*, 094509.
[25] M. E. Di Pietro, G. Celebre, G. De Luca, G. Cinacchi, *Phys. Rev. E* **2011**, *84*, 061703.
[26] M. E. Di Pietro, G. Celebre, G. De Luca, H. Zimmermann, G. Cinacchi, *Eur. Phys. J. E* **2012**, *35*, 112.